Chemical Science

ROYAL SOCIETY OF CHEMISTRY

EDGE ARTICLE

View Article Online
View Journal | View Issue

Cite this: *Chem. Sci.*, 2024, **15**, 9274

All publication charges for this article have been paid for by the Royal Society of Chemistry

Received 19th February 2024
Accepted 16th May 2024

DOI: 10.1039/d4sc01158a

rsc.li/chemical-science

Formation and reactivity of a unique M···C–H interaction stabilized by carborane cages†

Xin-Ran Liu,‡[a] Peng-Fei Cui,‡[a] Yago García-Rodeja,[b] Miquel Solà [b] and Guo-Xin Jin *[a]

Broadening carborane applications has consistently been the goal of chemists in this field. Herein, compared to alkyl or aryl groups, a carborane cage demonstrates an advantage in stabilizing a unique bonding interaction: M···C–H interaction. Experimental results and theoretical calculations have revealed the characteristic of this two-center, two-electron bonding interaction, in which the carbon atom in the arene ring provides two electrons to the metal center. The reduced aromaticity of the benzene moiety, long distance between the metal and carbon atom in arene, and the upfield shift of the signal of M···C–H in the nuclear magnetic resonance spectrum distinguished this interaction from metal···C π interaction and metal–C(H) σ bonds. Control experiments demonstrate the unique electronic effects of carborane in stabilizing the M···C–H bonding interaction in organometallic chemistry. Furthermore, the M···C–H interaction can convert into C–H bond metallization under acidic conditions or *via* treatment with *t*-butyl isocyanide. These findings deepen our understanding regarding the interactions between metal centers and carbon atoms and provide new opportunities for the use of carboranes.

Introduction

Icosahedral carboranes ($C_2B_{10}H_{12}$) are carbon–boron molecular clusters,[1] serving as useful building blocks in various applications.[2–7] The carborane substituents have been widely used to tune ligand properties. Because of the unique electronic effects of carboranes,[8–12] they are often recognized as three-dimensional inorganic benzene analogs.[13,14] Based on this property, many studies have explored compounds such as carborynes (1,2-dehydro-*ortho*-carboranes),[15] transition metal–carboryne complexes,[16] and *o*-carborane-fused borirans.[17] However, being a large steric, electron-deficient group, carborane also exhibits considerable differences compared to the benzene ring. These differences contribute to the stabilization of radicals[18–20] and intermediates.[21] However, whether carborane can stabilize specific bonding interactions is yet to be discovered. Currently, considerable effort in carborane chemistry is primarily devoted to the research of metal centers and B–H bonds.[22–27] The advantages of carborane itself in stabilizing special interactions, especially the metal···C–H interaction, are unclear and under investigation.

Because species containing a metal–arene bonding interaction are known to be the key intermediates in synthetic chemistry,[28–30] considerable efforts have been devoted to understanding this bonding interaction.[31,32] Among these species, the metal···C–H interaction of arenes is easily confused with other interactions, such as metal···C π interactions,[33,34] metal–C(H) σ bonds (Wheland intermediate),[29,35–37] metal···H–C agostic interactions,[38–40] and the van der Waals interactions[41] (Chart 1). Structural similarity and unclear concept of metal···C–H interaction are the root causes of this confusion. Moreover,

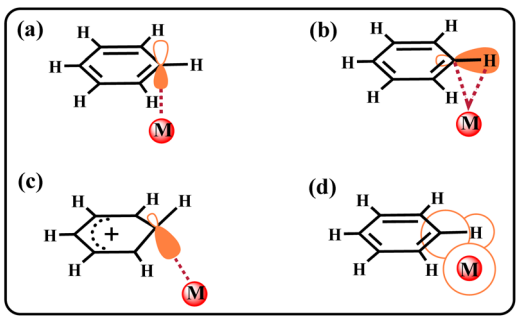

Chart 1 Examples of bonding interactions between a metal centre and arenes. The (a) metal···C π interaction, (b) metal···H–C agostic interaction, (c) metal–C(H) σ bond, and (d) van der Waals interaction.

[a]*State Key Laboratory of Molecular Engineering of Polymers, Shanghai Key Laboratory of Molecular Catalysis and Innovative Materials, Department of Chemistry, Fudan University, 2005 Songhu Road, Shanghai, 200433, P. R. China. E-mail: gxjin@fudan.edu.cn*

[b]*Institut de Química Computacional i Catàlisi, Departament de Química, Universitat de Girona, C/Maria Aurèlia Capmany, 69, 17003 Girona, Spain*

† Electronic supplementary information (ESI) available. CCDC 2303636 (complex **3b**), 2303637 (complex **3a**), 2303638 (complex **5a**), 2303639 (complex **6**), 2303640 (**L3**), 2303641 (complex **4**), 2303643 (**L4**) and 2303644 (complex **5b**). For ESI and crystallographic data in CIF or other electronic format see DOI: https://doi.org/10.1039/d4sc01158a

‡ X.-R. L. and P.-F. C. contributed equally to this paper.

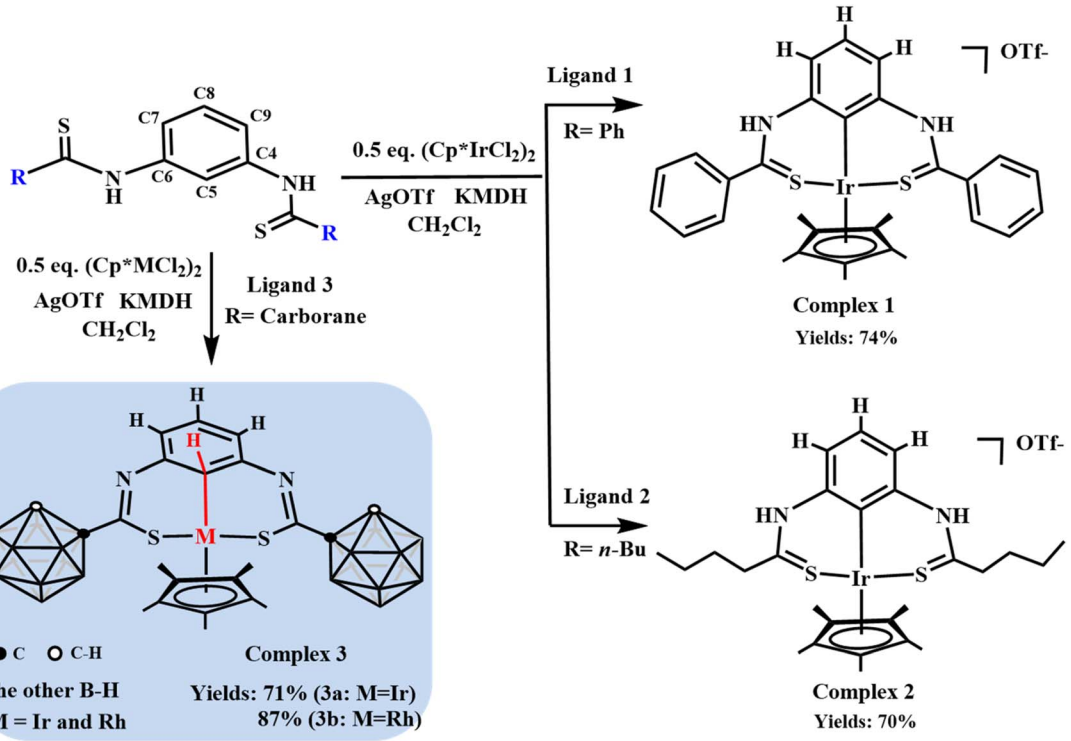

Scheme 1 Synthesis of complexes **1**, **2**, and **3**.

the unique M···C–H interaction is unstable and can easily metallize the C–H bond, making its stabilization more difficult. Therefore, the M···C–H interaction is mainly stabilized by additional intramolecular restraints. Such restraints can be introduced by incorporating the arene moiety into an appropriately sized macrocycle.[41,42] However, it is unclear whether the metal···C–H interaction can be stabilized by regulating the intramolecular electronic effect.[42] A clear definition of this bonding interaction has also not yet been proposed.

To investigate the stabilizing effect and bonding characteristics of the metal···C–H interaction, tridentate coordinating pincer-type ligands containing carborane, phenyl, or *n*-butyl groups were designed and synthesized. The results reveal that the special electronic effects of the carborane cage can stabilize this bonding interaction. Theoretical calculations were also performed to gain insights into the bonding model of this special metal···C–H interaction. Further investigations indicate that the unique metal···C–H interaction can achieve C–H bond activation under acidic conditions or in the presence of the strong coordination ligand *t*-butyl isocyanide (CN–Bu^t). These findings clearly define the characteristics of the metal···C–H interaction and broaden the prospect of carboranes in stabilizing special bonding interactions.

Results and discussion

Generally, the C–H bond of benzene in pincer-type ligands is easily activated by transition metals owing to strong chelation.[43] Therefore, obtaining the metal···C–H bonding interaction in such complexes is difficult. To address this challenge, different pincer-type ligands were designed and synthesized (for more details, see the ESI†). Further, the reactions of the synthesized pincer-type ligands with $[Cp^*MCl_2]_2$ (M = Ir or Rh) were explored (Scheme 1).

First, when ligand **1** was treated with $[Cp^*IrCl_2]_2$ (0.5 equiv.), followed by the addition of AgOTf and potassium bis(-trimethylsilyl)amide (KMDH), the ^{1}H nuclear magnetic resonance (NMR) spectrum of complex **1** showed no singlet peak corresponding to the C5–H proton and the Cp* signal was observed at 1.64 ppm (Fig. S1†). This indicated that the C5–H bond on the benzene ring was directly activated. The ^{19}F NMR spectrum of complex **1** showed a signal at −78.35 ppm (Fig. S6†), indicating the formation of an ionic complex; this result was also supported by electrospray ionization mass spectrometry (ESI-MS) analysis [$(M - OTF)^+$ = 675.1479; calc. 675.1456; Fig. S7†]. These results confirm the metallization of the C5–H bond. After failing to achieve the metal···C–H interaction using ligand **1**, it was determined if the interaction could be achieved by altering the electronic effects of the R group presented in Scheme 1. Then, ligand **2** was designed, where phenyl was replaced with *n*-butyl. However, a similar reaction as in case of ligand **1** occurred, forming complex **2**. The structure of complex **2** was further confirmed *via* NMR and ESI-MS analysis (Fig. S8, S10 and S14†). The signals of Cp* and the N–H proton were observed at 1.52 and 10.94 ppm in the ^{1}H NMR spectrum of complex **2** (Fig. S8†), respectively, indicating the presence of a C5–H bond-metallized complex such as complex **1**. The ESI-MS analysis results [$(M - OTF)^+$ = 635.2096; calc. 635.2083; Fig. S14†] also supported the formation of

complex **2**. These results indicate that the C–H bond of the benzene ring is easily activated in such a coordinated model.

To achieve the metal···C–H interaction, the charge density at the iridium center needs to be modified. Because phenyl and *n*-butyl can be considered as electron-donating groups, the effect of an electron-withdrawing group on the stability of the metal···C–H interaction needs to be explored. The carborane cage is a very competitive candidate as an electron-withdrawing group because of the electron deficiency of the B atom. Currently, carborane is used to stabilize radical complexes because of its large steric hindrance and unique electronic effects, but its use for stabilizing special bonding interactions is challenging. Ligand **3** was designed and reacted with $[Cp^*IrCl_2]_2$ (0.5 equiv.) under conditions similar to those of ligands **1** and **2** (Scheme 1 and Fig. 1). The ^{1}H NMR spectrum of complex **3a** shows a singlet corresponding to the C5–H proton, and this peak shifted upfield (from δ = 7.51 to 5.66 ppm) from the normal region for aryl protons in complex **3a** (Fig. 1c and d). This indicates that the metal···C–H interaction is observed in complex **3a**. The ^{13}C NMR spectra of complex **3a** also showed that the signal of C5 appeared at δ = 41.71 ppm, which is in contrast to the other carbon atoms in the benzene ring, exhibiting peaks at 118.83–159.92 ppm (Fig. S29†). No signal was observed in the ^{19}F NMR spectrum of complex **3a**, indicating the formation of neutral complex **3a**, consistent with the ESI-MS results [$(M + H)^+$ = 807.4387; calc. 807.4412; Fig. 1b]. These results support the presence of a strong interaction between the metal center and the carbon atom in arene. Notably, van der Waals interactions and metal···C π interactions do not exhibit this phenomenon.[44] Therefore, the NMR signal is one of the characteristic signals indicating the presence of the metal···C–H interaction. Furthermore, the NMR signals of the protons of C(7,9)–H were also shifted upfield from δ = 7.52 (in ligand 1) to 6.59 ppm (Fig. 1c and d). Additionally, cyclohexadienyl cations usually exhibit an absorption band at ~420 nm in ultraviolet-visible (UV-vis) spectra;[45] however, no corresponding resonance was observed for complex **3a** (Fig. S34†). This shows the difference between the M···C–H interaction and the M–C(H) σ bond. As mentioned above, the metal···C–H interaction exhibits unique characteristics and may be an important intermediate in synthetic chemistry. Moreover, it is easily confused with other similar bonding interactions. It was assumed whether it was possible to come to an inductive definition of this bond, which requires as complete a characterization as possible.

The X-ray single-crystal diffraction data of complex **3a** were collected. The structure of complex **3a** shows that the metal center remains trivalent and is coordinated with two S atoms, a Cp* ring, and a C5 atom (Fig. 1a). It indicates that the valence

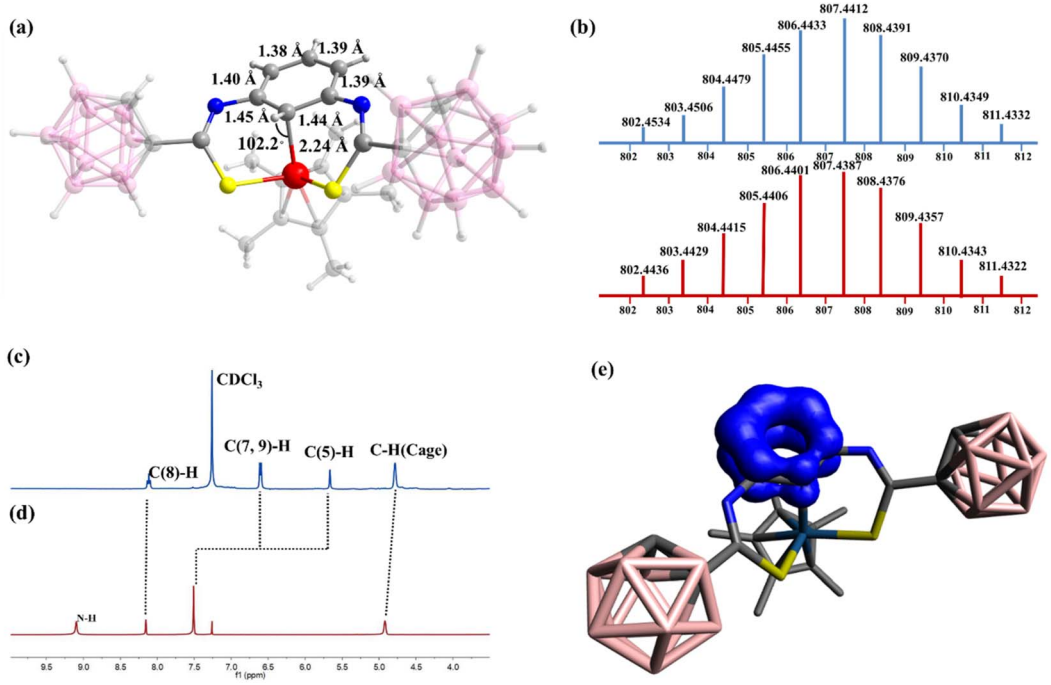

(f)	Total population of electrons	Total population of delocalized electrons
Benzene in 3a	36.66 e (6.11 e/atom)	3.52 e (0.59 e/atom)
Benzene	37.34 e (6.22 e/atom)	5.57 e (0.93 e/atom)

Fig. 1 (a) Molecular structure of complex **3a**: colour codes: Ir, red; S, yellow; N, blue; C, gray; B, pink; and H, light gray. The numbers indicate the bond lengths in the benzene ring and the angle of Ir–C5–H. (b) ESI-MS of complex **3a** (bottom: experimental; top: theoretical). Comparison of partial ^{1}H NMR ($CDCl_3$, 298 K) spectra of complex **3a** (c) and ligand **3** (d). The numbers indicate the carbon number on the benzene ring. (e) EDDB analysis of the complex **3a** and benzene ring. (f) Comparison of the total population of electrons (from EDDB charges in electrons) and delocalized electrons in benzene and in the benzene ring of complex **3a**.

state of the benzene ring does not change in M···C–H bonding type. However, as for M–C(H) σ bonding type, the carbon atom can be viewed as sp^3 carbon and the complex is a σ complex or Wheland intermediate. Thus, the benzene ring should be positive.[29,45] The lengths of the C5–C6 and C5–C4 bonds in **3a** are 1.45 and 1.44 Å, respectively, which are slightly longer than those of the other four bonds (~1.39 Å) (Fig. 1a). However, the lengths of the C5–C6 and C5–C4 bonds do not correspond to the length of a C–C single bond (1.54 Å). Additionally, the six carbon atoms in the benzene ring remain planar (but not in the M–C (H) σ bonding type[29,35]) and the angle of H–C5–Ir is 102.2° (Fig. 1a). These results suggest a considerable but not complete disruption of the aromaticity in the benzene ring of **3a**. Given the partial preservation of aromaticity, the Ir–C5 bond is expected to be somewhat longer than a comparable Ir–C σ bond. In line with this hypothesis, the observed Ir–C5 length of 2.24 Å (Fig. 1a) is consistent with the lengthening of the Ir–C σ bond (2.05 Å).

Natural bond order (NBO) analysis (Table S1†) verified the role of carboranes in stabilizing the M···C–H interaction. Because of the electron-withdrawing nature of the carborane cage, sulphur atoms exhibited lower charges (−0.089*e* and −0.121*e*) in ligand **3** than in ligands **1** and **2**, where S atoms had a charge of approximately −0.2*e*. Therefore, in ligands **1** and **2**, the lone pairs of electrons on the S atoms were more available for dative bonding compared with ligand **3**. These differences favoured the formation of a neutral structure for ligand **3** and cationic structures for ligands **1** and **2**. This is corroborated by the calculated Gibbs energies of the following reaction (see Fig. S66†):

$$\text{Complex n} + NEt_3H^+ \rightarrow \text{complex np} + NEt_3 \quad (1)$$

For ligand **3**, the C–H activation from complex **3a** is endergonic by 12.50 kcal mol^{-1}, whereas for ligands **1** and **2**, it is exergonic by 7.01 and 6.04 kcal mol^{-1}, respectively.

Density functional theory calculations provide insights into this bonding interaction. The three-center electron sharing index (3c-ESIs) value is close to zero, which indicates the absence of a three-centre bond in complex **3a** (see Table S4†).[46] Therefore, almost no interaction occurs between Ir and the H atom on C5. This illustrates that the M···C–H interaction is a two-centre bond, which differs from the three-center bond, metal···H–C agostic interaction. Table S4† gathers the results for complex **3a** and other types of interactions. M···C–H bond complexes are characterized by a relatively large M–C and a C–H bond order, a M–H bond order close to zero, and a relatively small 3c-ESI. The electron density of delocalized bonds (EDDB)

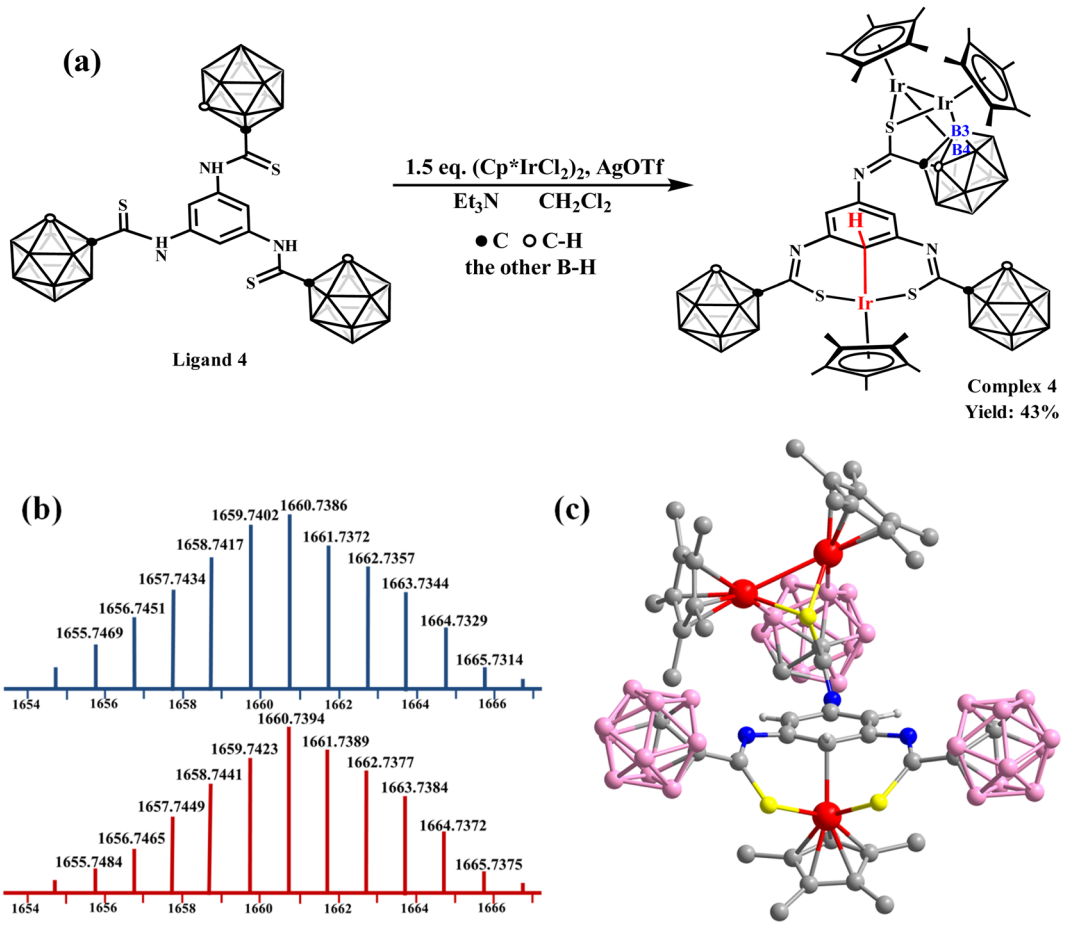

Fig. 2 (a) Synthesis of complex **4**. (b) ESI-MS of complex **4** (bottom: experimental; top: theoretical). (c) Molecular structure of complex **4**. Colour code: Ir, red; S, yellow; N, blue; C, gray; B, pink; H, light gray.

was computed to determine the influence of M···C–H interaction on the aromaticity of the benzene ring.[47] The delocalized electrons decreased from 5.6*e* for the benzene ring to 3.5*e* for complex **3a** (Fig. 1e and f and Table S2†). Moreover, the computed out-of-plane component of the nucleus-independent chemical shift (NICS(1)*zz*) corroborate the results obtained by EDDB, with NICS(1)*zz* = −19.9 ppm for complex **3a** and −27.7 for benzene (Table S3†). Therefore, the aromaticity of the benzene moiety is reduced but not completely disrupted. This is consistent with the aforementioned experimental results. To further understand the role of the C5 atom in this bonding interaction, NBO analysis was used,[48] which indicates that the Ir–C5 bond is formed through the interaction between the p-orbital of the C5 atom and the d-orbital ($5d_z^2$) of the Ir. With this interaction, the C5 atom can be viewed as providing a pair of electrons for iridium to satisfy the 18-electron rule. So far, the basic characteristics of the M···C–H interaction have been clearly characterized. Its characteristics can be summarized as follows: (1) the M···C–H interaction is a two-centre, two-electron bond, and the C atom provides a pair of electrons to the metal centre. (2) The aromaticity of the benzene moiety is reduced but not completely disrupted, causing a slight increase in the C–C bond length in the arene ring and metal–C interaction, but the six carbon atoms in the benzene ring remain planar. (3) Owing to the strong interaction between the metal centre and carbon atom in arene, the signal of M···C–H in the NMR spectrum shifts considerably upfield. These characteristics provide a way for identifying the M···C–H interaction. Similarly, this interaction can also be formed by reacting $[Cp^*RhCl_2]_2$ (0.5 equiv.) and ligand **3** (Scheme 1). The characteristics of complex **3b** have been described in detail in the ESI (Fig. S35–S42 and S69†).

Then, the ligand **4** was designed and synthesized to observe the effect of substituents on the benzene ring. The reaction of Ligand **4** with $[Cp^*IrCl_2]_2$ (1.5 equiv.) to form complex **4** in CH_2Cl_2 was explored (Fig. 2a). The ESI-MS analysis shows the synthesis of trinuclear complex **4** ($(M + H)^+$ = 1659.7423; calc. 1659.7402) (Fig. 2b). The ^1H NMR spectrum of complex **4** also exhibits a singlet at δ = 5.59 ppm (Fig. S43†), indicating M···C–H interaction formation. The X-ray single-crystal diffraction data of complex **4** confirm the unusual bonding pattern between the Ir center and C atom on one side and metallization of the B(3, 4) sites of the carborane cage on the other side (Fig. 2c). These results demonstrate that an M···C–H interaction can be stabilized by the carborane cage and is not affected by substituents on the *para*-position of the benzene ring.

After achieving the controlled formation of M···C–H interaction, its reactivities attract our attention. The first challenge is

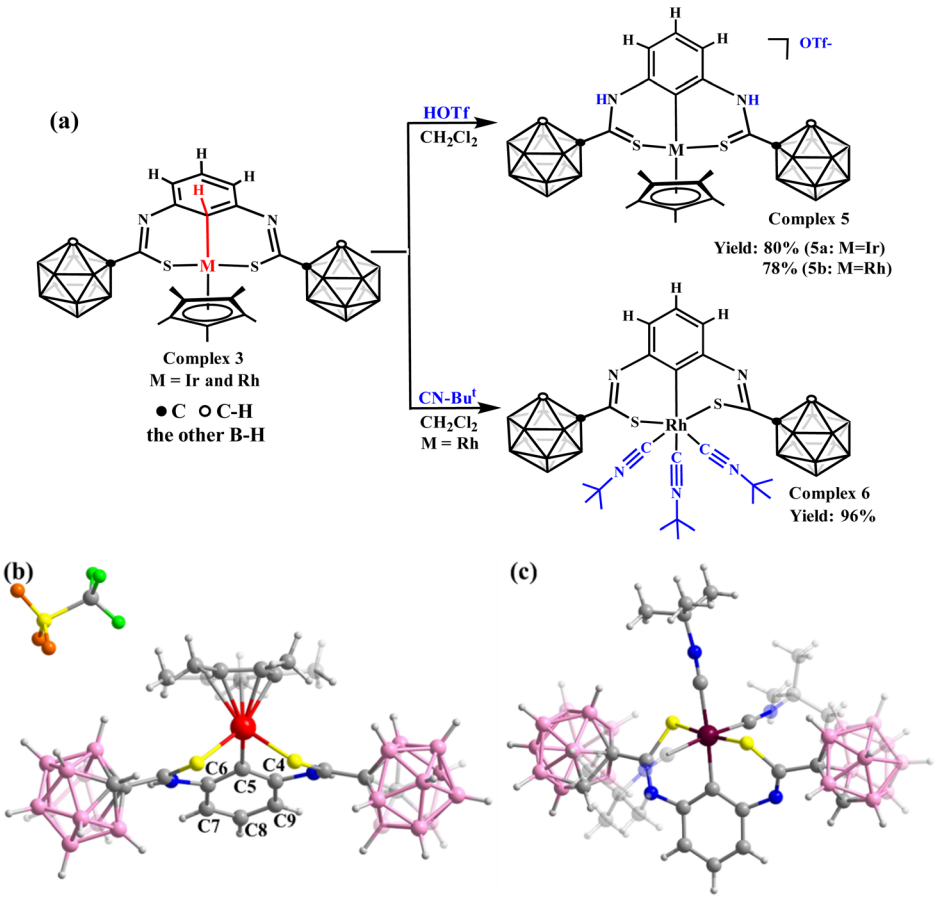

Fig. 3 (a) Reactivities of complex **3**. Molecular structure of complex **5a** (b) and complex **6** (c). Colour code: Ir, red; Rh, dark red; S, yellow; N, blue; C, gray; B, pink; H, light gray; O, orange; F, green. The notes show the carbon number on the benzene ring.

whether it can be converted into C–H metallization products. Compared with complexes **1**, **2**, and **3**, we found that if we could increase the charges of the S atoms, C–H bond metallization might be achieved. Hence, trifluoromethanesulfonic acid (HOTf) was added to complex **3** (Fig. 3a) to facilitate the formation of C=S bonds, increasing the charges of the S atoms. In the ^{1}H NMR spectrum of complex **5a**, the singlet signal of the C5–H bond in complex **3** disappeared, indicating C–H activation. The proton of the C–H peak from the remaining benzene ring appears at approximately $\delta = 6.78$ ppm (Fig. S48†). In the ^{13}C NMR spectrum (Fig. S50†), in contrast to complex **3a** ($\delta =$ 41.71 ppm), the signal of the carbon atom attached to Ir appears at $\delta = 108.35$ ppm. The bond lengths of the C5–C6 and C5–C4 bonds are 1.40 and 1.39 Å (Fig. 3b), slightly shorter than those in complex **3a** (1.43 Å and 1.44 Å). Moreover, the benzene ring in complex **5a** exhibits considerable rotation (Fig. 1a and 3b), reducing the length of the Ir–C5 bond (2.24 Å in complex **3a** and 2.05 Å in complex **5a**) and activating the C–H bond.

The abovementioned strategies to achieve C–H activation require changing the C–S bond to a C=S bond. This raises the question of whether C–H bond activation can be achieved while retaining the C–S single bond. To achieve this, the oxidation state or coordination configuration of the metal centre must be changed. However, complex **3** dissociates when an oxidizer (I_2) is added to it. This shows that C–H bond metallization cannot be achieved by changing the oxidation state of the metal centre. Subsequently, we applied a strong electron-donor ligand, CN–Bu^{t}. When CN–Bu^{t} is added to complex **3b**, the Cp* ring leaves to form complex **6** (Fig. 3a). However, a similar reaction did not occur in complex **3a**, possibly due to the stronger affinity of the Ir centre to the Cp* ring. The crystal structure of complex **6** (Fig. 3c) confirms that C–H-bond activation also causes a rotation of the benzene ring compared to complex **3**. These results again illustrate the importance of charge density at the metal centre in stabilizing the M···C–H interaction.

Conclusions

In this study, compared to alkyl or aryl groups, the carborane cage presents a unique application prospect in stabilizing special chemical bonding interactions. Owing to the importance of the M···C–H interaction in synthetic chemistry, this interaction was characterized in detail through single-crystal analysis, NMR spectroscopy, UV-vis spectroscopy, ESI-MS analysis, and theoretical calculations to provide a definition of this interaction. This would also effectively reduce the confusion of the metal···C–H interaction with other interactions. The analysis of this bonding interaction type can help deepen our understanding of the interactions between a metal centre and carbon atoms and is beneficial to understand the C–H bond activation process.

Data availability

Data supporting this study is available in the ESI† and further details are available from the authors on reasonable request.

Author contributions

Xin-Ran Liu and Peng-Fei Cui contributed equally to this work. Xin-Ran Liu and Peng-Fei Cui designed and synthesized all the compounds. Guo-Xin Jin supervised the research. Yago García-Rodeja and Miquel Solà performed theoretical calculations. All authors discussed the results and revised the manuscript.

Conflicts of interest

There are no conflicts to declare.

Acknowledgements

This work was supported by the National Science Foundation of China (22031003, 22201043) and the Shanghai Science Technology Committee (19DZ2270100). P. F. C. thanks the China Postdoctoral Science Foundation (BX2021073, 2021M700801). M. S. and Y. G. R. are grateful to the Spanish Ministerio de Ciencia, Innovación y Universidades (MICIU/AEI/10.13039/501100011033) for projects PID2020-113711GB-I00 and the "European Union-Next Generation" Maria Zambrano grant to Y. G.-R., and the Generalitat de Catalunya for project 2021SGR623.

Notes and references

1 R. N. Grimes, *Carboranes*, Elsevier, Oxford, 3rd edn, 2016, pp. 283–502, ISBN: 978-0-12-801894-1.
2 (*a*) A. Saha, E. Oleshkevich, C. Viñas and F. Teixidor, *Adv. Mater.*, 2017, **29**, 1704238; (*b*) J. Ochi, K. Tanaka and Y. Chujo, *Angew. Chem., Int. Ed.*, 2020, **59**, 9841–9855.
3 F. Issa, M. Kassiou and L. M. Rendina, *Chem. Rev.*, 2011, **111**, 5701–5722.
4 (*a*) D. Zhao and Z. Xie, *Coord. Chem. Rev.*, 2016, **314**, 14–33; (*b*) P. F. Cui, Y. Gao, S. T. Guo, Y. J. Lin, Z. H. Li and G. X. Jin, *Angew. Chem., Int. Ed.*, 2019, **58**, 8129–8133.
5 (*a*) B. J. Eleazer, M. D. Smith, A. Popov and D. V. Peryshkov, *J. Am. Chem. Soc.*, 2016, **138**, 10531–10538; (*b*) J. N. H. Reek, B. de Bruin, S. Pullen, T. J. Mooibroek, A. M. Kluwer and X. Caumes, *Chem. Rev.*, 2022, **122**, 12308–12369; (*c*) C. T. McTernan, J. A. Davies and J. R. Nitschke, *Chem. Rev.*, 2022, **122**, 10393–10437; (*d*) R. Banerjee, D. Chakraborty and P. S. Mukherjee, *J. Am. Chem. Soc.*, 2023, **145**, 7692–7711.
6 P. F. Cui, X. R. Liu, Y. J. Lin, Z. H. Li and G. X. Jin, *J. Am. Chem. Soc.*, 2022, **144**, 6558–6565.
7 P. F. Cui, X. R. Liu and G. X. Jin, *J. Am. Chem. Soc.*, 2023, **145**, 19440–19457.
8 I. B. Sivaev, *Comprehensive Organometallic Chemistry IV*, Elsevier, Amsterdam, 2022, vol. 9, pp. 196–262, ISBN: 9780128202067.
9 D. S. Tu, H. Yan, J. Poater and M. Solà, *Angew. Chem., Int. Ed.*, 2020, **59**, 9018–9025.
10 (*a*) A. M. Spokoyny, C. W. Machan, D. J. Clingerman, M. S. Rosen, M. J. Wiester, R. D. Kennedy, C. L. Stern, A. A. Sarjeant and C. A. Mirkin, *Nat. Chem.*, 2011, **3**, 590–596; (*b*) R. R. Huang, C. Wang, D. Tan, K. Wang, B. Zou,

Y. T. Shao, T. H. Liu, H. N. Peng, X. G. Liu and Y. Fang, *Angew. Chem., Int. Ed.*, 2022, **61**, e202211106.
11 X. R. Liu, P. F. Cui, S. T. Guo, Y. J. Lin and G. X. Jin, *J. Am. Chem. Soc.*, 2023, **145**, 8569–8575.
12 J. Poater, C. Viñas, I. Bennour, S. Escayola, M. Solà and F. Teixidor, *J. Am. Chem. Soc.*, 2020, **142**, 9396–9407.
13 Y. N. Ma, H. Ren, Y. Wu, N. Li, F. Chen and X. Chen, *J. Am. Chem. Soc.*, 2023, **145**, 7331–7342.
14 H. Y. Ren, P. Zhang, J. K. Xu, W. L. Ma, D. S. Tu, C. S. Lu and H. Yan, *J. Am. Chem. Soc.*, 2023, **145**, 7638–7647.
15 H. L. Gingrich, T. Ghosh, Q. R. Huang and Jr and M. Jones, *J. Am. Chem. Soc.*, 1990, **112**, 4082–4083.
16 Z. Qiu, S. Ren and Z. Xie, *Acc. Chem. Res.*, 2011, **44**, 299–309.
17 H. Zhang, J. Y. Wang, W. G. Yang, L. B. Xiang, W. C. Sun, W. B. Ming, Y. X. Li, Z. Y. Lin and Q. Ye, *J. Am. Chem. Soc.*, 2020, **142**, 17243–17249.
18 K. Jaiswal, N. Malik, B. Tumanskii, G. Ménard and R. Dobrovetsky, *J. Am. Chem. Soc.*, 2021, **143**, 9842–9848.
19 S. Li and Z. Xie, *J. Am. Chem. Soc.*, 2022, **144**, 7960–7965.
20 L. B. Xiang, J. Y. Wang, I. Krummenacher, K. Radacki, H. Braunschweig, Z. Y. Lin and Q. Ye, *Chem.–Eur. J.*, 2023, **29**, e202301270.
21 (*a*) S. Kim, J. W. Treacy, Y. A. Nelson, J. A. M. Gonzalez, M. Gembicky, K. N. Houk and A. M. Spokoyny, *Nat. Commun.*, 2023, **14**, 1671; (*b*) S. L. Yao, A. Saddington, Y. Xiong and M. Driess, *Acc. Chem. Res.*, 2023, **56**, 475–488.
22 Y. Quan and Z. Xie, *Chem. Soc. Rev.*, 2019, **48**, 3660–3673.
23 X. Zhang and H. Yan, *Coord. Chem. Rev.*, 2019, **378**, 466–482.
24 Y. Baek, S. Kim, J. Y. Son, K. Lee, D. Kim and P. H. Lee, *ACS Catal.*, 2019, **9**, 10418–10425.
25 F. R. Lin, J. L. Yu, Y. J. Shen, S. Q. Zhang, B. Spingler, J. Y. Liu, X. Hong and S. Duttwyler, *J. Am. Chem. Soc.*, 2018, **140**, 13798–13807.
26 L. Yang, B. B. Jei, A. Scheremetjew, R. Kuniyil and L. Ackermann, *Angew. Chem., Int. Ed.*, 2021, **60**, 1482–1487.
27 (*a*) W. Y. Man, D. Ellis, G. M. Rosair and A. J. Welch, *Angew. Chem., Int. Ed.*, 2016, **55**, 4596–4599; (*b*) Y. N. Ma, Y. Gao, Y. B. Ma, Y. Wang, H. Ren and X. Chen, *J. Am. Chem. Soc.*, 2022, **144**, 8371–8378.
28 M. Brookhart, M. L. H. Green and G. Parkin, *Proc. Natl. Acad. Sci. U.S.A.*, 2007, **104**, 6908–6914.
29 A. J. Canty and G. V. Koten, *Acc. Chem. Res.*, 1995, **28**, 406–413.
30 W. D. Jones, *Activation of Unreactive Bonds and Organic Synthesis*, ed. S. Murai, H. Alper, R. A. Gossage, V. V. Grushin, M. Hidai, Y. Ito, W. D. Jones, F. Kakiuchi, G. Koten, Y. S. Lin, Y. Mizobe, S. Murai, M. Murakami, T. G. Richmond, A. Sen, M. Suginome and A. Yamamoto, Springer Berlin, Heidelberg, 1999, pp. 9–46, ISBN: 978-3-642-08436-2.
31 W. H. Bernskoetter, C. K. Schauer, K. I. Goldberg and M. Brookhart, *Science*, 2009, **326**, 553–556.
32 J. D. Watson, L. D. Field and G. E. Ball, *Nat. Chem.*, 2022, **14**, 801–806.
33 C. C. Li, Z. Chen, Y. M. Huang, Y. R. Zhang, X.-Y. Li, Z. W. Ye, X. Xu, S. E. J. Bell and Y. K. Xu, *Chem*, 2022, **8**, 2514–2528.
34 S. Filipuzzi, P. S. Pregosin, M. J. Calhorda and P. J. Costa, *Organometallics*, 2008, **27**, 2949–2958.
35 M. Albrecht, R. A. Gossage, A. L. Spek and G. V. Koten, *J. Am. Chem. Soc.*, 1999, **121**, 11898–11899.
36 D. M. Grove, G. V. Koten, J. N. Louwen, J. G. Noltes, A. L. Spek and H. J. C. Ubbels, *J. Am. Chem. Soc.*, 1982, **104**, 6609–6616.
37 T. Steinke, B. K. Shaw, H. Jong, B. O. Patrick, M. D. Fryzuk and J. C. Green, *J. Am. Chem. Soc.*, 2009, **131**, 10461–10466.
38 X. H. Lin, W. Wu and Y. R. Mo, *Coord. Chem. Rev.*, 2020, **419**, 213401.
39 P. L. Arnold, A. Prescimone, J. H. Farnaby, S. M. Mansell, S. Parsons and N. Kaltsoyannis, *Angew. Chem., Int. Ed.*, 2015, **54**, 6735–6739.
40 S. Murugesan, B. Stçger, E. Pittenauer, G. Allmaier, L. F. Veiros and K. Kirchner, *Angew. Chem., Int. Ed.*, 2016, **55**, 3045–3048.
41 M. Stepien, L. Latos-Grazynski, L. Szterenberg, J. Panek and Z. Latajka, *J. Am. Chem. Soc.*, 2004, **126**, 4566–4580.
42 (*a*) X. Ribas, C. Calle, A. Poater, A. Casitas, L. Gómez, R. Xifra, T. Parella, J. Benet-Buchholz, A. Schweiger, G. Mitrikas, M. Solà, A. Llobet and T. D. P. Stack, *J. Am. Chem. Soc.*, 2010, **132**, 12299–12306; (*b*) C. Lepetit, J. Poater, E. Alikhani, B. Silvi, Y. Canac, J. Contreras-García, M. Solà and R. Chauvin, *Inorg. Chem.*, 2015, **54**, 2960–2969; (*c*) M. Montag, L. Schwartsburd, R. Cohen, G. Leitus, Y. Ben-David, J. M. L. Martin and D. Milstein, *Angew. Chem., Int. Ed.*, 2007, **46**, 1901–1904.
43 Y. L. Wang, Z. D. Huang, G. X. Liu and Z. Huang, *Acc. Chem. Res.*, 2022, **55**, 2148–2161.
44 J. C. Ma and D. A. Dougherty, *Chem. Rev.*, 1997, **97**, 1303–1324.
45 (*a*) D. M. Brouwer, E. L. Mackor and C. MacLean, *Carbonium Ions*, ed. G. A. Olah and P. V. Schleyer, Wiley-Interscience, New York, 1970, pp. 837–897, ISBN978-1-4684-8541-7; (*b*) R. Rathore, J. rgen Hecht and J. K. Kochi, *J. Am. Chem. Soc.*, 1998, **120**, 13278–13279.
46 Y. Garcıa-Rodeja, F. Feixas, E. Matito and M. Solà, *Phys. Chem. Chem. Phys.*, 2022, **24**, 29333–29337.
47 D. W. Szczepanik, M. Andrzejak, J. Dominikowska, B. Pawełek, T. M. Krygowski, H. Szatylowicz and M. Solà, *Phys. Chem. Chem. Phys.*, 2017, **19**, 28970–28981.
48 A. E. Reed, L. A. Curtiss and F. Weinhold, *Chem. Rev.*, 1988, **88**, 899–926.